Histological, Spectroscopic, and Surface Analysis of Microdamage in Bone: Toward Real-Time Analysis Using Fluorescent Sensors

Raman Parkesh,*[,†,‡] Sahar Mohsin,[‡] T. Clive Lee,[‡] and Thorfinnur Gunnlaugsson[†]

School of Chemistry, Centre for Synthesis and Chemical Biology, Trinity College Dublin, Dublin 2, Ireland, and Department of Anatomy, Royal College of Surgeons in Ireland, St. Stephen's Green, Dublin 2, Ireland

Received October 25, 2006. Revised Manuscript Received January 19, 2007

This paper describes the characterization of microdamage in bones histologically, spectroscopically, and by surface analysis. A set of fluorescent (photoinduced electron transfer, PET) sensors, bearing phenyliminodiacetate moieties as ion receptors, was used to investigate the selective labeling of microdamage in bones, which can have significant value for analysis of bone structures in humans. Scratched and unscratched surfaces of the bone were studied using fluorescence microscopy, Raman spectroscopy, SEM, and EDXA. These results were compared to those using Rose Bengal dye. The overall results show that selective labeling of scratches occurred for all the fluorescent sensors, which can be attributed to the interaction of dyes via binding at free lattice sites (via the receptors), through ionic interactions with free lattice sites or by incorporation in the broken lattices. The principal mode of operation is most likely due to the binding of these sensors to Ca(II) at microdamage sites.

Introduction

Bone is a rigid but dynamic organ that undergoes continuous repair, molding, and shaping. As bone is under constant stress due to repetitive loading during normal day-to-day activity, this results in the generation of microcracks or microdamage.[1] These fatigue-related microcracks that range in length from 25 to 300 μm have been observed in vivo in human, canine, bovine, ovine, and rat bone.[2] Histology is the most common method used for studying the quantity and characteristics of damage responsible for mechanical degradation. It has been shown that microdamage in bone acts as a stimulus for bone remodeling.[3] This remodeling is mediated by the well-balanced actions of osteoclasts, which initiate old bone resorption, and osteoblasts, which form new bone.[3] Bulk staining of bones with basic fuchsin was the first dye used by Frost[2] to label in vivo microdamage and was soon established as the method of choice for differentiating cracks generated during dehydration, sectioning, and polishing from those existing in the tissue prior to processing.[4] However, this method suffers from a number of disadvantages such as nonuniform staining and underestimation of quantification of microdamage; this method is also not suitable for labeling submicroscopic damage.[5] Lee et al.[6−7] introduced a novel idea for sequential labeling of microdamage in bone by using five colorimetric agents: Calcein, Xylenol orange, Alizarin complexone, Calcein blue, and Oxytetracycline. Microcracks were made visible under an epifluorescence microscope. However, these dyes suffer from a number of disadvantages, such as limited aqueous solubility, high pKa value, low affinity for Ca(II) at neutral pH, and high intrinsic fluorescence.[8] Consequently, there exists a need for improving on this technique, particularly with the aim of developing noninvasive methods for analysis of bone structures for medical diagnostics. In the past, we have been involved in the development of both lanthanide luminescent and fluorescent photoinduced electron transfer (PET) sensors as well as colorimetric sensors for biologically relevant anions and cations.[9] Thus, we set out to investigate the possibility of using (i) new fluorescent chemosensors, designed in our laboratory; (ii) commercially available sensors, or probes; and (iii) synthetic iodinated contrast agents to detect bone damage.[10,11] Here, the objective was to use these sensors to selectively visualize bone damage. The current study reports the application of commercially available fluorescent (PET) sensors, such as calcium crimson, calcium orange, and fluo-3 (Figure 1) to label surface

* Corresponding author. E-mail: raman.parkesh@pharm.ox.ac.uk.
† Trinity College Dublin.
‡ Royal College of Surgeons in Ireland.

(1) (a) Jee, W. S. S. In *A Textbook of Histology*; Weiss, L., Ed.; Urban Schwarzenberg: Baltimore, 1988; Chapter 7.
(2) Frost, H. M. *Henry Ford Hosp. Bull.* **1960**, *8*, 35.
(3) (a) Frost, H. M. In *Bone Remodelling and its Relationship to Metabolic Bone Diseases*; Charles C. Thomas: Springfield, IL, 1973. (b) Lee, T. C.; Staines, A.; Taylor, D. *J. Anat.* **2002**, *201*, 437. (c) Martin, R. B.; Burr, D. B. *Structure, Function and Adaptation of Compact Bone*; Raven Pres: New York, 1989. (d) Giladi, M.; Milgrom, C.; Simkiu, A.; Danon, Y. *Am. J. Sports Med.* **1991**, *19*, 647. (e) Burr, D. B.; Martin, R. B.; Schaffler, M. B.; Radin, E. L. *J. Biomech.* **1985**, *18*, 189. (f) Martin, R. B. *J. Orthop. Res.* **1995**, *13*, 309.
(4) (a) Forwood, M. R.; Parker, A. W. *Calcif. Tissue. Int.* **1989**, *45*, 47. (b) Burr, D. B.; Stafford, T. *J. Biomech. Eng.* **1999**, *121*, 616. (c) Burr, D. B.; Hooser, M. *Bone* **1995**, *17*, 431.
(5) (a) Boyce, B. F.; Byars, J.; McWilliams, S.; Mocan, M. Z.; Elder, H. Y.; Boyle, I. T.; Junor, B. J. R. *J. Clin. Pathol.* **1992**, *45*, 502. (b) Lee, T. C.; Myers, E. R.; Hayes, W. C. *J. Anat.* **1998**, *193*, 179.
(6) Lee, T. C.; Arthur, T. L.; Gibson, L. J.; Hayes, W. C. *J. Orthop. Res.* **2000**, *18*, 322.
(7) (a) O'Brien, F. J. *Microcracks and the Fatigue Behavior of Compact Bone*. Ph.D. Thesis, University of Dublin, Dublin, Ireland, 2000. (b) O'Brien, F. J.; Taylor, D.; Lee, T. C. *J. Biomech.* **2002**, *35*, 523.
(8) (a) Wänninen, E. In *Indicators*; Bishop, E., Ed.; Pergamon Press: New York, 1971; p 231. (b) Huitink, G. M. *Talanta* **1987**, *34*, 423. (c) Wilkins, D. H.; Hibbs, L. E. *Talanta* **1959**, *2*, 201. (d) Wallach, D. F. H.; Surgenor, D. M.; Soderberg, J.; Delano, E. *Anal. Chem.* **1959**, *31*, *456*. (e) Escarilla, A. M. *Talanta* **1966**, *11*, 363. (f) Wallach, D. F. H.; Steck, T. L. *Anal. Chem.* **1963**, *35*, 1035.

10.1021/cm0625427 CCC: $37.00
Published on Web 03/07/2007

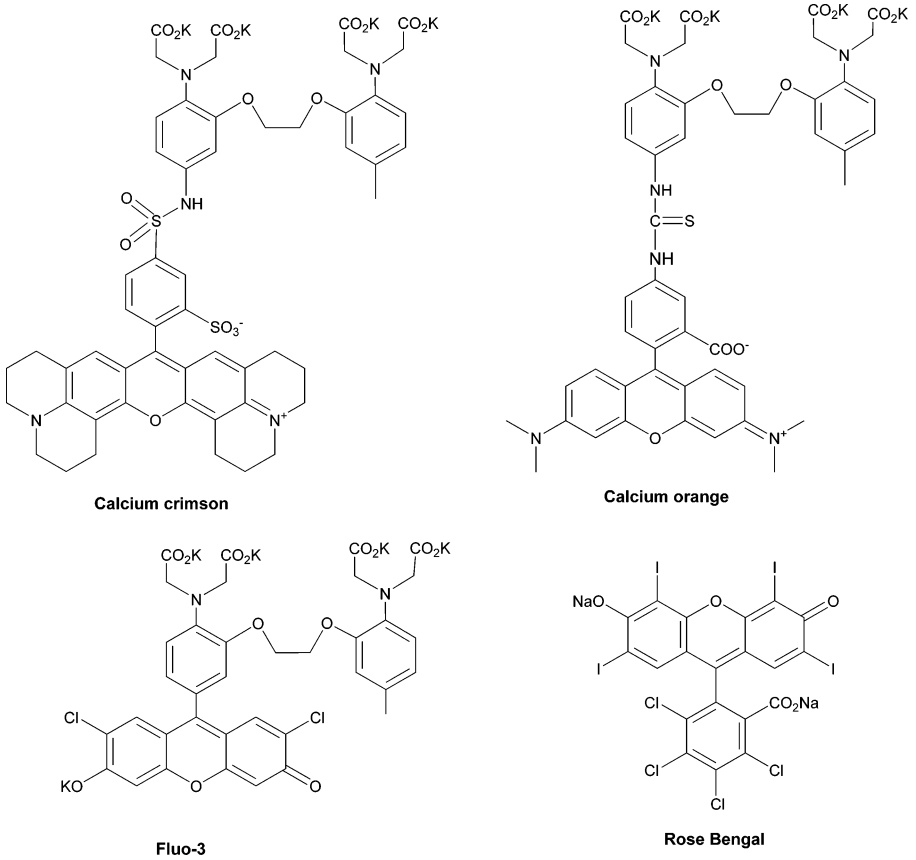

Figure 1. Structure of PET sensors and Rose Bengal used in the current study.

scratches in a reproducible model of microdamage in bones. These dyes have the advantage of high water solubility, pH independence in the physiological range, and being nonfluorescent in the absence of calcium.[12,13] Rose Bengal, a dye containing iodine atoms, was used to obtain further insights into the mechanisms of microdamage labeling of these PET sensors, by using fluorescence microscopy (epifluorescence studies) Raman spectroscopy and energy-dispersive X-ray analysis (EDXA). The crystallization of Rose Bengal in the microcracks demonstrates the benefit of using chelating dyes for labeling microdamage. Here we give the results of the latter of these investigations.

Experimental Section

Epifluorescence Studies of Bone Specimens using Calcium Crimson, Fluo-3, and Calcium Orange. The dyes were purchased from Molecular Probes Ltd. Fluo-3 and calcium orange were received as potassium salts. Calcium crimson was obtained as its ethyl ester derivative and was hydrolyzed prior to use. The ethyl ester was dissolved in 5 mL of methanol; 1 mL of 3 M aqueous KOH was added to it, and the reaction mixture was refluxed for 2 h. The solvent was evaporated and the resulting residue extracted into water and precipitated upon the addition of ethanol. A solution (1×10^{-4} M) of each dye was prepared in buffer solution (pH = 7.4, 20 mM HEPES, 135 mM KCl to maintain constant ionic strength). Bovine tibiae were obtained from a meat wholesaler (KEPAK Ltd., Clonee, Co. Dublin) from animals slaughtered 2−3 days previously. The soft tissue was removed from all bones and

(9) (a) Senechal-David, K.; Leonard, J. P.; Plush, S. E.; Gunnlaugsson, T. *Org. Lett*. **2006**, *8*, 2727. (b) McCoy, C. P; Stomeo, F.; Plush, S. E.; Gunnlaugsson, T. *Chem. Mater*. **2006**, *18*, 4336. (c) Gunnlaugsson, T.; Leonard, J. P.; Sénéchal, K.; Harte, A. J. *J. Am. Chem. Soc*. **2003**, *125*, 12062. (d) Gunnlaugsson, T.; Kruger, P. E.; Jensen, P.; Tierney, J.; Ali, H. D. P.; Hussey, G. M. *J. Org. Chem.* **2005**, *70*, 10875. (e) Gunnlaugsson, T.; Leonard, J. P. *Chem. Commun.* **2003**, 2424. (f) Gunnlaugsson, T.; Ali, H. D. P.; Glynn, M.; Kruger, P. E.; Hussey, G. M.; Pfeffer, F. M.; dos Santos, C. M. G.; Tierney, J. *J. Fluoresc.* **2005**, *15*, 287. (g) Gunnlaugsson, T.; Kruger, P. E.; Lee, T. C.; Parkesh, R.; Pfeffer, F. M.; Hussey, G. M. *Tetrahedron Lett.* **2003**, *44*, 6575. (h) Gunnlaugsson ,T.; Davis, A. P.; Hussey, G. M.; Tierney, J.; Glynn, M. *Org. Biomol. Chem.* **2004**, *2*, 1856. (i) Gunnlaugsson, T.; Lee, T. C.; Parkesh, R. *Org. Lett.* **2003**, *5*, 4065. (j) Gunnlaugsson, T.; Lee, T. C.; Parkesh, R. *Org. Biomol. Chem.* **2003**, *19*, 3265. (k) Gunnlaugsson, T.; Lee, T. C.; Parkesh, R. *Tetrahedron* **2004**, *60*, 11239. (l) Gunnlaugsson, T.; Harte, A. J.; Leonard, J. P.; Nieuwenhuyzen, M. *Supramol. Chem.* **2003**, *13*, 505.

(10) (a) Parkesh, R.; Gowin, W.; Lee, T. C.; Gunnlaugsson, T. *Org. Biomol. Chem.* **2006**, *4*, 3611. (b) Parkesh, R.; Lee, T. C.; Gunnlaugsson, T.; Gowin, W. *J. Biomech.* **2006**, *39*. 1552−1556.

(11) Parkesh, R. Ph.D. Dissertation, University of Dublin, Dublin, Ireland, 2003.

(12) (a) Tsien, R. Y. *Methods Enzymol.* **1999**, *20*, 224. (b) Tsien, R. Y. *Annu. Rev. Neurosci.* **1989**, *12*, 227. (c) Tsein, R.Y. In *Fluorescent Chemosensors for Ion and Molecular Recognition*; ACS Symposium Series 538; Czarnik, A. W., Ed.; American Chemical Society: Washington, D.C., 1993; p 130. (d) Valeur, B. In *Topics in Fluorescence Spectroscopy, Vol. 4: Probe Design and Chemical Sensing*; Lakowicz, J. R., Ed.; Plenum Press: New York, 1994; p 22. (e) Kuhn, M. A. In *Fluorescent Chemosensors for Ion and Molecular Recognition*, ACS Symposium Series 538; Czarnik, A. W., Ed.; American Chemical Society: Washington, D.C., 1993; p 47. (f) Ramaswami, M.; Krishnan, K. S.; Kelly, R. B. *Neuron* **1994**, *13*, 363. (g) Sinha, S. R.; Patel, S. S.; Saggu, P. *J. Neurosci. Methods* **1995**, *60*, 49. (h) Canepari, M.; Mammano, F. *J. Neurosci. Methods* **1999**, *87*, 1.

(13) (a) Horobin, R. W. In *Conn's Biological Stains, A Handbook of Dyes, Stains and Fluorochromes for Use in Biology and Medicine*, 10th ed.; Horobin, R. W., Kiernan, J. A., Eds.; BIOS Scientific Publishers Ltd.: Oxford, U.K., 2002; p 203. (b) Martini, F. H.; Ober, W. C.; Garrison, C. W.; Welch, K.; Hutchings, R. T. *Fudamentals of Anatomy and Physiology*, 5th ed; Prentice Hall: Upper Saddle River, NJ, 2001; Chapter 6.

these were stored at −20 °C until required. Longitudinal sections of cortical bone from the mid-diaphysis were cut into beams using a band saw and polished using emery paper (grade 400). All machining was carried out in wet conditions and the bones were not allowed to dry at any time. After machining, the specimens were stored at −20 °C prior to staining. A 5 mm straight line was scratched on the surface of each of the bone sample using a compass point. Samples were dipped into a 1×10^{-4} M buffered solution of each PET sensor in an individual vial, which was placed under a vacuum (50 mmHg) for intervals of 5, 15, 30, and 60 min. Specimens were washed in deionized water. For substitution tests, specimens were washed in deionized water; a new line of the same length was drawn parallel to the earlier one and the specimen was then reimmersed in the buffered solution of the PET sensor. These bone specimens were then examined using UV epifluorescence ($\lambda = 365$ nm) and green epifluorescence ($\lambda = 546$ nm). Images were captured using a CCD color video camera and analyzed using the image software Lucia.

Raman Imaging Studies using Calcium Crimson, Calcium Orange, and Rose Bengal. Longitudinal sections of bovine tibiae were prepared in the manner previously described. For comparison purposes, specimens without any scratches as well as unlabeled scratched bone specimens were analyzed. The bone samples were immersed into the solution of each fluorophore (1×10^{-4} M) in individual vials and placed under a vacuum (50 mm of Hg) for 24 h. The samples were washed with deionized water, dried, and then analyzed. These samples were compared with unscratched and scratched controls. The Labram system, comprising a confocal Raman imaging microscope and an argon ion laser sources (514.5 nm, 50 mW) was used. The 1004 cm^{-1} band of toluene was scanned before the acquisition of the resonance Raman spectra, to ensure correct positioning of the monochromator. The monochromator was stepped using increments of 0.5 cm^{-1}. For calibration purposes, the Raman spectrum of acetonitrile was recorded and peak frequencies and intensities adjusted until it agreed with reported values. A variable objective focused the line-shaped laser beam onto the bone surface and scratch. The scattered light was collected by an objective in a confocal geometry and dispersed onto an air-cooled CCD array by one of two interchangeable gratings, 1800 or 600 lines/mm allowing the range from 150 cm^{-1} to 4000 cm^{-1} to be covered in a single image, or with greater resolution in a combination of images. With the former, a spectral resolution of 1 cm^{-1} per pixel is achievable. The data were analyzed using LabView (National instruments Corp.) software. Data were corrected for baseline offset and processed using a filter to remove cosmic events and artefactual spikes. These studies were conducted at the Dublin Institute of Technology, Ireland.

SEM and EDXA Studies of Bone Samples using Rose Bengal. The protocol used for EDXA studies was similar to that used in Raman imaging studies and is shown in the above section. Rose Bengal was used for EDXA and SEM studies, as it has a carboxylic group that can bind to the scratch and iodine atoms that can be analyzed by EDXA. All SEM micrographs were obtained with a dual stage SEM with associated EDXA and samples coated with gold to achieve optimal SEM images. For EDXA analysis, uncoated samples were used. Studies were conducted using unscratched, scratched, and Rose Bengal-labeled bone specimens and were carried at the Centre for Microscopy and Analysis, Trinity College Dublin.

Results and Discussion

Fluorescence Imaging Studies. The receptors in the above dyes (the phenyliminodiacetate moieties) are multidentate ligands that have chelating groups organized in three dimensions, which we have previously used successfully in the synthesis of X-ray contrast agents.[10,11] This allows the chelating agent to be highly dependent on the size and charge of the metal ion and as such is extremely ion selective. The use of the BAPTA chelator ensures that the pKa of the receptor does not overlap with the physiological pH range, so that weakly acidic conditions will not provide a false positive response via protonation.[11,12] Furthermore, the fluorophores do not contain any ionizable groups in the pH range of 7−8. Because the potassium salts of these indicators are used, they possess high water solubility as well as high stability. Moreover, the long excitation wavelength used reduces any interference from autofluorescence (e.g., from bone proteins such as collagen and from light scattering).[12,13a] The dyes have high extinction coefficients[12] and thus absorb strongly in the visible region, which permits a lower dye concentration to be used in order to prevent phototoxicity to bones and bone cells when applied in vivo.

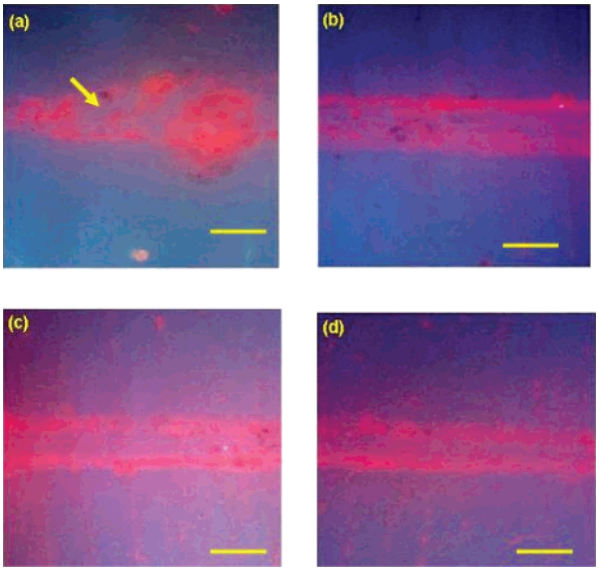

Figure 2. Epifluorescence micrograph of bone surface showing a scratch labeled with calcium crimson at different time intervals: (a) 5, (b) 15, (c) 30, and (d) 60 min; bar = 100 μm, UV epifluorescence excitation at 365 nm.

The epifuorescent images for bones stained with a 1×10^{-4} M solution of calcium crimson as a function of time are shown in Figure 2. The images clearly show that the scratches are selectively and exclusively labeled with the dye, and that there is little difference in the brightness of the labeled scratch as a function of time, indicating efficient and fast absorption of these dyes in the scratched areas. This was supported by qualitative analysis, which showed that increasing the immersion time did not lead to any significant improvement in the color nor the intensity beyond 15 min. Thus 15 min was deemed the optimal immersion time for the investigations carried out herein for all the sensors. The bright pink/red fluorescent color of the dye in Figure 2 provided a good contrast from the blue autofluorescence observed from the collagen proteins of bone. The strong emission also indicates that the sensors have high affinity for the damaged (scratched) areas, which is important for diagnostics. It is hypothesized that the scratched area consisted of coordinatively unsaturated

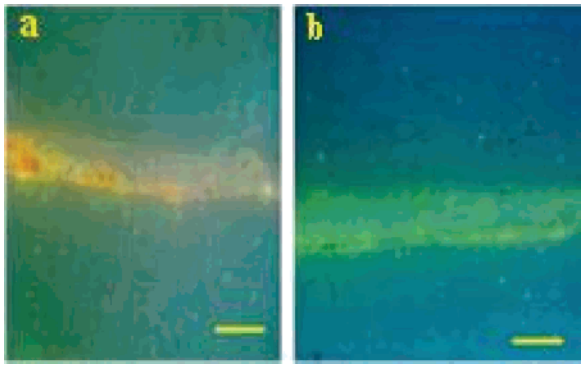

Figure 3. Epifluorescence micrograph of bone surface showing scratch labeled with (a) calcium orange and (b) fluo-3; bar = 200 μm, UV epifluorescence excitation at 365 nm.

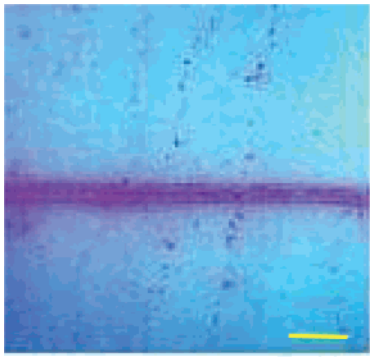

Figure 4. Bone surface showing scratch labeled with Rose Bengal; UV epifluorescence (365 nm). Bar = 500 μm.

Ca(II) that is available for binding by the phenyliminodiacetate moieties. Calcium crimson is known to have high affinity toward Ca(II).[13] Outside the scratched areas, the emission of these sensors is only minor (*switched off*), indicating that the sensors do not bind there. Moreover, the emission from the sensors would be expected to be minor in the absence of Ca(II) because of effective PET quenching of the flourophore by the receptor.[14] However, upon binding of the receptor at the damaged site (scratch), the receptor cannot participate in any photoinduced electron-transfer PET quenching of the flourophore and the emission would be enhanced or *'switched on'*. This occurs as the Ca(II) recognition increases the oxidation potential of the receptors, which makes the electron transfer thermodynamically unfavorable. Indeed, Figure 2 shows this to be the case. The other important advantage is that the dye is highly water soluble and so buffered solutions can be readily prepared. The images were also analyzed under different magnifications (see the Supporting Information), which clearly demonstrated that calcium crimson was able to label the bone scratch in its entirety without affecting the surrounding area of the bone.

Similar results were obtained with calcium orange, fluo-3, and Rose Bengal. Here, the orange fluorescence (Figure 3a) and the green fluorescence (Figure 3b) were observed for the first two dyes, respectively, upon excitation at 365 nm. As before, both of these dyes were able to label the scratch selectively and effectively, making the scratched clearly area distinguishable from the surrounding area of the bone specimens. This clearly demonstrates the selectivity of the receptor for the exposed, or free, Ca(II) in the scratches, and that these sensors also function as PET sensors. Again, the blue background fluorescence of the bone matrix (autofluorescence) is easily differentiated.

In contrast to these results, Rose Bengal, used as its sodium salt, did not give rise to as striking a contrast between the scratched bone matrix and the background in the same manner as the previous three sensors. Even though Rose Bengal has many attractive features, such as good solubility in water (36%, w/v) and low pKa (3.9 and 4.7)[13] for the carboxylate and hydroxyl groups, respectively, rendering it pH independent in the physiological range, the bright pink color of the dye was not as clearly visible in the scratched area of the bone. Structurally, the dye is different from the fluorescence sensors discussed above, as it lacks the phenyliminodiacetate moieties, having instead the aforementioned single benzoic acid receptor. This reduces considerably the binding affinity of Rose Bengal with Ca(II) relative to the other sensors descibed above. Nevertheless, the scratch is visible, which demonstrates that the dye has higher affinity for the scratch rather than the surrounding bone matrix. These important results demonstrate that a dye capable of forming weak interactions can also specifically label the scratch (Figure 4). However, for potential clinical use, such a marginal color change is not ideal, and of the four dyes analyzed herein, calcium crimson would be have the greatest potential for clinical application. However, these results demonstrate selective affinity of these sensors for the cracks, which also indicates that the cracks are rich in chelatable calcium, which on binding to the chelating groups of the sensors switches the fluorescence on. Having established that all the dyes were able to detect the cracks in the bone matrix, we set out to evaluate the nature of the binding of these dyes to the cracks. As explained above, all the fluorescent dyes are PET sensors, and as such, the emission would ideally only be switched on upon binding of the receptor to free Ca(II) sides.[14]

Evaluation of Substitution Tests with Calcium Crimson, Calcium Orange and Fluo-3. From our previous work,[11] the dissociation constants (K_d) for Ca(II) for the fluorescent sensors investigated above follow the order of calcium crimson (203 nM) < calcium orange (423 nM) < fluo-3(3900 nM). Therefore, if these dyes are to be applied in a sequence of decreasing binding affinity, no substitution is expected to occur. To verify this hypothesis, we performed substitution tests using a three dye sequence, in concentration of 1×10^{-4} M. The results obtained are shown in a series of paralled scratches (Figure 5), where it can be seen that the three-dye sequence resulted in no substitution or mixing and that the three dyes are clearly distinct both from each other and the surrounding bone matrix. This sequence could be of help in identifying a propagating microcrack in bone.

As bone is a complex material[13,15] that consists of canals, Haversian systems, cell lacunae, canaliculi, and resorption

(14) de Silva, A. P.; Gunaratne, H. Q. N.; Gunnlaugsson, T.; Huxley, A. J. M.; McCoy, C. P.; Rademacher, J. T.; Rice, T. E. *Chem. Rev.* **1997**, *97*, 1515.

(15) Frost, H. M. *Introduction to a New Skeletal Physiology, Vol. I and II*; Pajaro Group: Pueblo, CO, 1995.

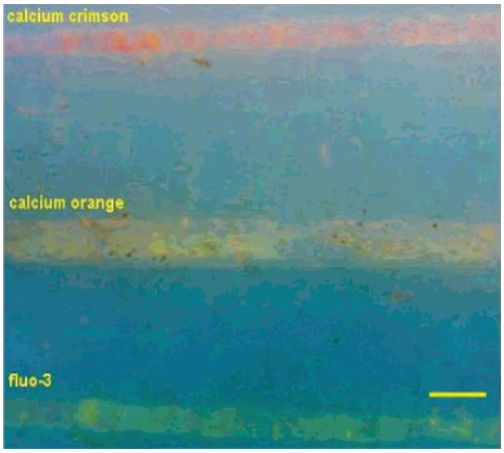

Figure 5. Three-dye sequence for analyzing the substitution pattern: calcium crimson, calcium orange, and fluo-3; UV epifluorescence (365 nm), bar = 200 μm.

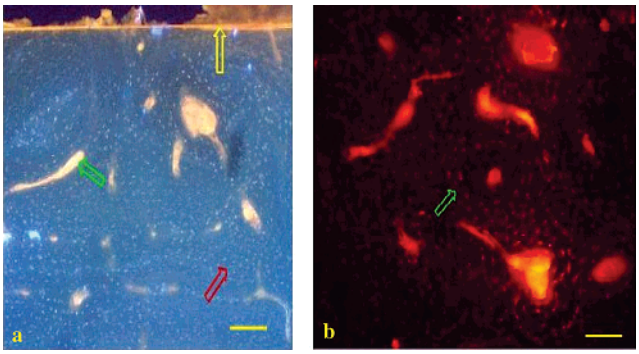

Figure 6. Transverse section of bone labeled with calcium orange in (a) UV epifluorescence microscopy (365 nm) and (b) green epifluorescence microscopy excitation (546 nm). Yellow arrow = bone surface; red arrow = cell lacuna. Green arrow shows bone canal in image a and osteon with its cell lacunae, canaliculi and central Haversian canal in image b. Bar = 100 μm.

cavities, dyes that have the ability to penetrate the bone matrix are of considerable importance for gaining an understanding of this complex morphology. For this purpose, a penetration test as described in the Experimental Section was conducted. Figure 6 shows the UV and green epifluorescence images of a transversely sectioned bone specimen stained with calcium orange. It is clear from Figure 6 that calcium orange is able to bind selectively with different surfaces in bone. The area marked with green, yellow, and red arrows in Figure 6a are the bone canals, bone surface, and the bone cell lacunae, respectively. All these components contain suitable coordinatively unsaturated Ca(II) binding sites to facilitate the binding and the reduction/removal of the PET quenching from the receptor (upon complexation to the Ca(II)) to the flourophore. This gives rise to the concomitant enhancement in fluorescence. The internal structure of the bone comprising osteons and interstital lamellae are also clearly visible when viewed under green epifluorescence, by excitation at 546 nm, as is evident from Figure 6b. To further understand this and quantify the selective labeling of the scratch generated on a bone surface, two additional techniques were explored, namely the use of Raman confocal microscopy and Energy Dispersive X-ray Analysis (EDXA) coupled with a Scanning Electron Microscopy (SEM).

Raman Spectroscopic Analysis of Bones in the Presence and Absence of Calcium Crimson, Calcium Orange, and Rose Bengal Labeled Bone Samples. Raman spectroscopy[16] will provide information about the microstructure of bone at a molecular level under physiological conditions in a noninvasive manner. It provides information-rich spectral bands, is insensitive to water and noninvasive, and sample preparation is very easy.[17] It was reasoned that the comparison of the Raman spectra of the surrounding bone, scratches, and labeled scratches would give new insights into the mechanism by which the sensors bind not to the bone surface and only to the scratched area.

Each unscratched and unlabeled bone specimen was first scanned to obtain a background Raman spectrum. This spectrum was further processed by subtraction of baseline and filtration of the data. This dramatically improved the signal-to-noise ratio and led to background removal (Figure 7a). The spectrum shows the presence of eight prominent Raman bands. Bands observed at 430 and 589 cm^{-1} were assigned to the vibrations of phosphate groups (ν_4) of the hydroxyapatite lattice, respectively. The most prominent band, observed at 961 cm^{-1}, is also due to the phosphate (ν_1).

A weak intensity band observed at ca. 857 cm^{-1} can be assigned to either carbonate frequency or to the C−C stretch of proline and hydroxyproline. Vibrations of bone proteins are responsible for the bands appearing at 1249, 1455, and 1667 cm^{-1}, respectively.[17,18] Having obtained the background, we next measured the Raman spectra of the scratched surface of the bone (Figure 7b). The spectrum is similar to that shown in Figure 7a, except that there are distinct changes in the bands in the region of 1000−1100 cm^{-1}, where two separate bands can be observed at 1000 and 1046 cm^{-1}, respectively. These bands were assigned to the phosphate of the hydroxyapatite lattice of the bone, which is now more exposed, and can be attributed to the breakage of the phosphate bonds in the hydroxyapatite lattice during scratch generation. This is backed by the fact that degradation studies carried out on collagen proteins have demonstrated extensive perturbation in the amide bonds observed at 1250 and 1660 cm^{-1}.[19] However, in the present case, no changes were observed in the 1200−1600 cm^{-1} range, indicating that collagen proteins were intact during scratch generation.

The most interesting results, however, were obtained when the bone specimens were labeled with the fluorescence sensors calcium crimson and calcium orange, respectively. For both dyes, the scratched region and the surrounding

(16) (a) Raman, C. V.; Krishnan, K. S. *Nature* **1928**, *121*, 501. (b) Raman, C. V. In *Nobel Lectures (Physics)*; Elsevier: New York, 1965; p 267. (c) Chantry, G. W. In *The Raman Effects, Volume 1: Principles*; Anderson, A., Ed.; Marcel Dekker: New York, 1979.
(17) (a) Pelletier, M. J. In *Analytical Applications of Raman Spectroscopy*; Pelletier, M. J., Ed.; Blackwell Science Ltd.: Malden, MA, 1999; p 1. (b) Malyj, M.; Griffiths, J. E. *J. Appl. Spectrosc.* **1983**, *37*, 315. (c) Rassat, S. D.; Davis, E. *J. Appl. Spectrosc.* **1994**, *48*, 1498.
(18) (a) Timlin, J. A.; Carden, A.; Morris, M. D.; Rajachar, R, M.; Kohn, D. H. *Anal. Chem.* **2000**, *72*, 2229. (b) Carden, A.; Rajachar, R, M.; Morris, M. D.; Kohn, D. H. *Calcif. Tissue Int.* **2003**, *72*, 166. (c) Wutheir, R E. *Connect. Tissue Res.* **1989**, *22*, 27. (d) Penel, G.; Leroy, G.; Bres, E. *J. Appl. Spectrosc.* **1998**, *53*, 312.
(19) Paschalis, E. P.; Verdelis, K.; Doty, S. B.; Boskey, A. L.; Mendelsohn, R.; Yamauchi, M. J. *Bone Miner. Res.* **2001**, *16*, 1821.

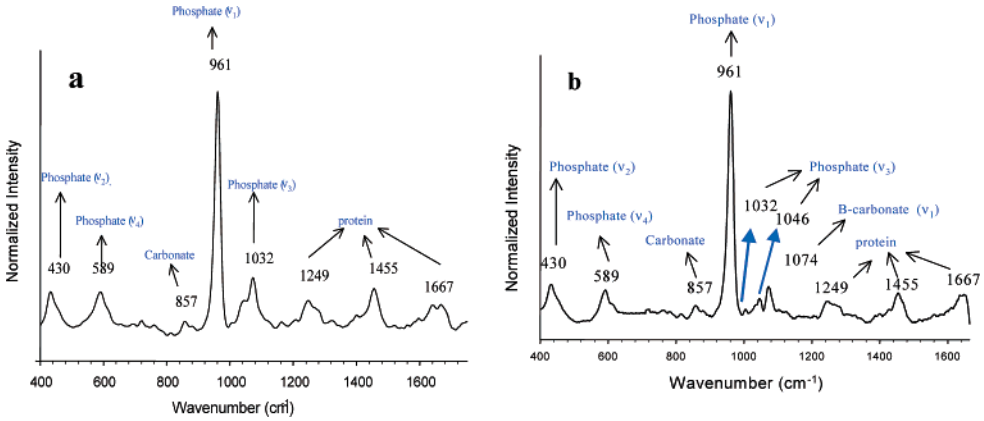

Figure 7. Corrected Raman spectra of (a) unscratched and unlabeled bone and (b) scratched and unlabeled regions of bone. Both spectra have been normalized to phosphate $\nu_1 = 1$.

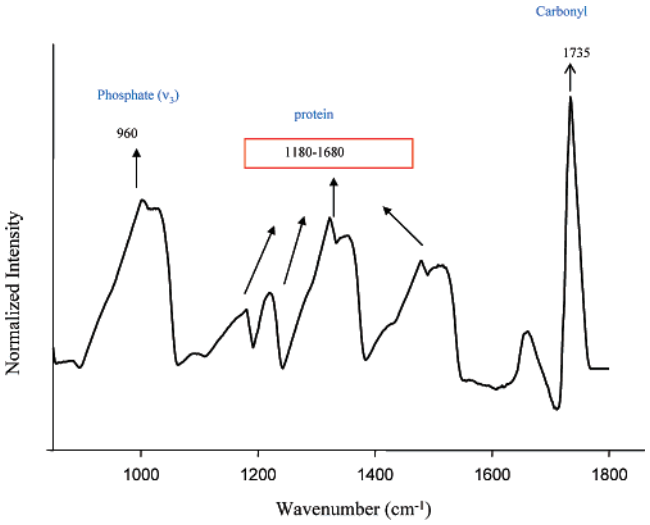

Figure 8. Corrected Raman spectrum of the bone scratch labeled with calcium crimson. The spectrum has been normalized to phosphate $\nu_1 = 1$.

unscratched surfaces were scanned and analyzed. For these, the Raman spectra of the unscratched surface were identical to that shown in Figure 7a, whereas the Raman spectrum of the scratch labeled with Calcium crimson, depicted in Figure 8, was significantly different. Here, a broad phosphate band centered at 1001 cm^{-1} is clearly observed. The bands appearing in the region 1180−1400 cm^{-1} can be assigned to the amide vibration of collagen proteins and to the aromatic region of the sensor itself. The amide and CH_2 stretching are also clearly represented by the bands observed within the 1450−1680 cm^{-1} region. The most striking and high-intensity band, however, is the one center at 1735 cm^{-1}, which is most likely due to the carbonyl groups of the calcium crimson sensor. The Raman spectrum of the unscratched region was almost identical to that of the unlabeled and unscratched bone specimen, clearly showing that the sensor has bound selectively to the scratched area and supporting our finding from the fluorescence measurements discussed above. Similar results were obtained using calcium orange. Unfortunately, in the case of Rose Bengal, the spectrum was dominated by high signal-to-noise ratio and background noise, making the interpretation of Raman bands almost impossible (see the Supporting Information). This behavior of organic pigments is a well-known phenomenon

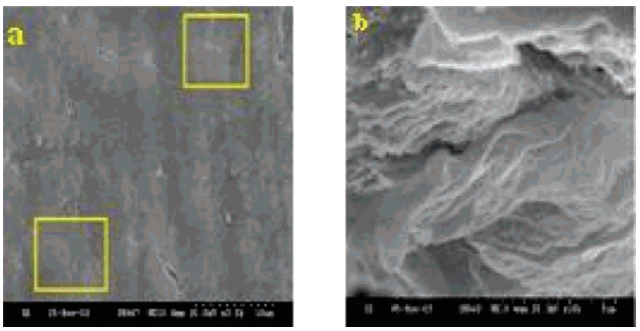

Figure 9. Scanning electron micrograph of (a) intact and (b) scratched bone. Two different regions (marked by a yellow rectangle in a) were selected for elemental composition by EDXA.

in Raman spectroscopy.[20] The most likely reason may be the presence of pigment impurities and the higher energy absorption of the dye at 514 nm laser excitation. The Raman frequency data clearly provide the evidence of chemical changes in the scratch and thus support our above findings that selective labeling of these sensors within the scratched areas is indeed the reason for the high fluorescence intensity seen in the microscopy studies.

Scanning Electron Microscopy (SEM) and Energy-Dispersive X-ray Analysis (EDXA) of Bone Samples Labeled with Rose Bengal. The sensor chosen for the labeling of bone samples for these experiments was the Rose Bengal dye, as it has a high iodine atom content; the dye can be observed in the EDXA spectrum, which enables the labeled scratch to be distinguished from the surrounding hydroxyapatite matrix. As a background, a SEM picture of the unscratched sample is shown in Figure 9, for comparison. Chemical composition analysis of this bone sample was performed using EDXA (see the Supporting Information). Because of the highly composite nature of the bone matrix, two different regions were selected for elemental analysis. The EDXA spectra indicates that the major elements present in bone are, as expected, calcium, phosphorus, and oxygen, along with trace amounts of sodium, magnesium, and phosphorus. Additionally, the elemental compositions of both chosen regions were identical, within experimental error. This result demonstrates that the bone exhibits chemical unifor-

(20) Bell, S. E. J.; Bourguignon, E. S.; O'Grady, A.; Villaumie, J.; Dennis, A. C. *Spectrosc. Eur.* **2002**, *14*, 17.

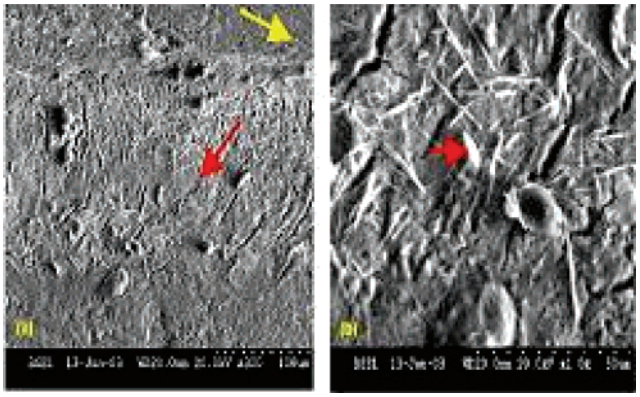

Figure 10. Scanning electron micrograph of scratched bone labeled with Rose Bengal at (a) low resolution and (b) high resolution. Red arrows show the Rose Bengal crystallized in the scratch area. Yellow arrow shows the area surrounding scratch.

mity. Moreover, the elemental composition of the scratch was also within experimental error, identical with the surrounding bone matrix. The scanning electron micrograph demonstrates the morphology of the damaged lattice. It shows the highly porous nature of the scratched area caused by the breaks in the hydroxyapatite lattice.

The EDXA pictures of the bones labeled with Rose Bengal are shown in Figure 10 and provided interesting results. The SEM of the scratched area clearly showing the formation of crystals within the scratched region which we believe is the coordinated form of Rose Bengal. Hence, whereas the dye is clearly visible in the scratch, no crystals are detected in the surrounding matrix. This result supports our finding above, that even though the binding to Ca(II) might be relatively week, it does occur within the damaged area of the bone. It can also be postulated that the porous and void nature of the broken lattice in the scratch induces crystallization of the dye. This further supports the proposal that the sensors target only the more exposed surface of the bone matrix and hence can be used selectively to target microdamage in bones. Moreover, the EDXA analysis, for these measurements, Figure 11, further supports this argument, as it is possible to detect the presence of high iodine content (Figure 11b) in the scratch and not in the unscratched bone matrix (Figure 11a). This further supports the fact that Rose Bengal is present only in the scratch. It can thus be concluded that the SEM and the EDXA findings support the epifluorescence and Raman imaging studies carried out and discussed above and confirm that the sensors can selectively target the exposed Ca(II) in the scratch areas.

Conclusion

We have carried out a detailed and comprehensive analysis of the ability of three fluorescent sensors to selectively target scratches in a bone. This is an important investigation for both the use of such sensors as a histological method and establishing the possibility of using fluorescent PET sensors for medical use in noninvasive bone imaging. To evaluate the histological findings, we also explored two independent techniques, Raman spectroscopy and SEM-coupled EDXA.

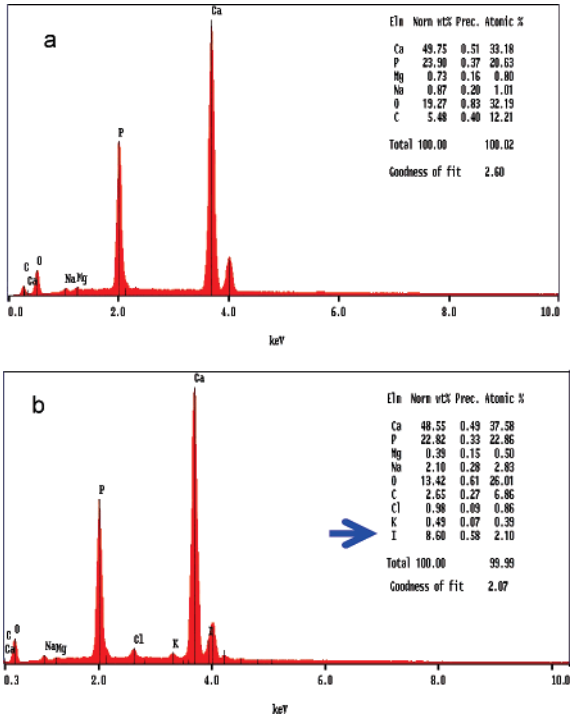

Figure 11. Elemental composition of (a) surrounding area and (b) scratched area of bone labeled with Rose Bengal; the blue arrow in part b shows the iodine composition in the scratched region.

The results from these investigations show that it was possible to understand the difference between the scratched and unscratched surfaces of the bone in terms of lattice vibrations (using Raman spectroscopy) using commercially available fluorescent sensors designed for Ca(II) detection. Importantly, these results also showed that the sensors were able to specifically label the scratched areas rather than the surrounding regions of the bone. We believe that the reason for this is that the generation of a scratch breaks this mineral lattice and generates lattice vacancies for bound elements, such as Ca(II), that will be able to bind suitable receptor functionalities. Further evidence for such binding/chelation was obtained by carrying our SEM and EDX analysis of Rose Bengal-labeled scratches showing the selective crystallizations of dye in the scratch. It demonstrates that even suitable ionic interactions can be exploited for selective scratch labeling. We can thus conclude that for the selective labeling of the sensors investigated herein, their imaging in the bone cracks is probably due to either their chelation at the free Ca(II) vacant sites generated during scratching or inhibition of the PET process via interaction with the porous lattice. These results will have implications in studying in vivo microfractures in bone, as the sensor will penetrate microdamage sites and bind to coordinatively unsaturated Ca(II). As a result, microdamage would be visible by epifluoresence and other techniques. The nanomolar level affinity of these sensors for free Ca(II) will facilitate selective labeling of microdamge sites. We are further investigating these phenomena in detail using atomic force microscopy (AFM) and extended X-ray absorption fine structure (EXAFS), with the aim of understanding the selectivity better

and determining the binding mode and geometry adapted by the dye in the scratch in greater detail.

Acknowledgment. We gratefully acknowledge financial support from The Health Research Board of Ireland, Trinity College Dublin, and the Royal College of Surgeons in Ireland. We also thank Dr. Rethi Madathil and Dr. Chunnu from the Chemistry Department, Oxford University, for helpful discussions, Dr. Hugh Byrne from Focas, Ireland, for Raman Spectroscopy measurements, and Mr. Neal Leddy for assistance with SEM and EDX measurements. We thank anonymous reviewers for helpful comments.

Supporting Information Available: Bone epifluorescent pictures with calcium orange at different magnification, Raman spectrum of Rose Bengal, EDXA element composition of intact and scratched bone. This material is available free of charge via the Internet at htpp://pubs.acs.org.

CM0625427